The Role of ^{89}Zr-Immuno-PET in Navigating and Derisking the Development of Biopharmaceuticals

Guus A.M.S. van Dongen, Wissam Beaino, Albert D. Windhorst, Gerben J.C. Zwezerijnen, Daniela E. Oprea-Lager, N. Harry Hendrikse, Cornelis van Kuijk, Ronald Boellaard, Marc C. Huisman, and Danielle J. Vugts

Department of Radiology and Nuclear Medicine, Amsterdam University Medical Centers, Vrije Universiteit Amsterdam, Amsterdam, The Netherlands

The identification of molecular drivers of disease and the compelling rise of biotherapeutics have impacted clinical care but have also come with challenges. Such therapeutics include peptides, monoclonal antibodies, antibody fragments and nontraditional binding scaffolds, activatable antibodies, bispecific antibodies, immunocytokines, antibody–drug conjugates, enzymes, polynucleotides, and therapeutic cells, as well as alternative drug carriers such as nanoparticles. Drug development is expensive, attrition rates are high, and efficacy rates are lower than desired. Almost all these drugs, which in general have a long residence time in the body, can stably be labeled with ^{89}Zr for whole-body PET imaging and quantification. Although not restricted to monoclonal antibodies, this approach is called ^{89}Zr-immuno-PET. This review summarizes the state of the art of the technical aspects of ^{89}Zr-immuno-PET and illustrates why it has potential for steering the design, development, and application of biologic drugs. Appealing showcases are discussed to illustrate what can be learned with this emerging technology during preclinical and especially clinical studies about biologic drug formats and disease targets. In addition, an overview of ongoing and completed clinical trials is provided. Although ^{89}Zr-immuno-PET is a young tool in drug development, its application is rapidly expanding, with first clinical experiences giving insight on why certain drug–target combinations might have better perspectives than others.

Key Words: ^{89}Zr-immuno-PET; monoclonal antibodies; biopharmaceuticals; antibody–drug conjugates; immune checkpoint inhibitors

J Nucl Med 2021; 62:438–445
DOI: 10.2967/jnumed.119.239558

The completion of the Human Genome Project in 2003 boosted the identification of disease targets and the development of targeted drugs, as well as introducing the concept of personalized therapy. Nevertheless, it is fair to state that new-drug development remains challenging with respect to number of approvals, quality of innovation, and cost effectiveness. About 10 y ago, 20–30 new molecular entities were approved each year. At that time, research-and-development productivity, defined as the relationship between the value (medical or commercial) created by new medicines and the investment required to generate those medicines, was considered to be the critical factor to be improved, as advocated by Paul et al. in 2010 (*1*). They identified 2 productivity-limiting steps: the first is that drug development is expensive (the average costs to bring a single drug to the market was estimated to be near $1 billion), and the second is that research and development are inefficient and take a long time (only 8% of clinical candidate drugs make it to approval, and this process takes more than 10 y). Attrition rates are highest for drugs in early-phase clinical trials, whereas costs are highest when drugs fail in late-stage clinical trials.

After efficiency, the next important factor in research-and-development productivity is effectiveness, being the distinguished clinical value of a drug. In this factor, also, much is desired, considering that even registered drugs are effective in only a portion of patients. To reduce phase II and III attrition, Paul et al. proposed 2 key approaches (*1*): the first is to have better target selection (i.e., the selection of more validated and druggable targets), and the second is the use of biomarkers, especially in phase I, that ensure target engagement or predict and evaluate efficacy and toxicity.

THE EMERGING ROLE OF BIOLOGICALS

The number of drug approvals increased from an average of 30 per year in 2000–2013 to about 50 per year after that time (*2*). One reason was the increase in biologicals, particularly monoclonal antibodies (mAbs). The share of biologicals among the new U.S. Food and Drug Administration (FDA)–approved drugs was about 25% from 2010 to 2013 and 47% from 2014 to 2018 (*3*). These comprised hormones, clotting factors, enzymes, vaccines, nucleic acid products, engineered cell-based products, and especially mAbs (50% share). With 570 antibodies at various clinical stages in 2019, including 62 in late-stage clinical studies, continuation of these trends can be expected for the coming years (*4*). In 2018, the share of biologicals was $251 billion of the worldwide drug market, valued at about $1,000 billion/y, and it is expected to reach $625 billion in 2026. Despite these dizzying numbers, the success rate to reach drug approval remained almost constant at around 10%. These are overall figures, and it should be realized that drug development in certain disease areas such as mental or brain diseases is even less successful, confirming the difficulty of research and development in these areas (*5*).

POTENTIAL ROLE OF ^{89}ZR-IMMUNO-PET

Motivated by these trends, ^{89}Zr-immuno-PET was developed by our group for PET imaging of mAbs and clinically applied for the first time in 2006 (*6*). At that time, most approved mAbs were conventional IgG molecules, mostly used as antagonists for

Received Sep. 17, 2020; revision accepted Dec. 1, 2020.
For correspondence or reprints contact: Guus A.M.S. van Dongen, De Boelelaan 1117, 1081 HV Amsterdam, The Netherlands.
E-mail: gams.vandongen@amsterdamumc.nl
Published online Dec. 4, 2020.

selective inhibition of receptor tyrosine kinases or to modulate or block other critical membrane targets in cancer and other diseases. The safety and therapeutic success of these first-generation mAbs have stimulated the development of next-generation mAb constructs, which have increased potency, have multiple binding domains, or bind to novel targets such as immune checkpoints. Among others, these constructs comprise antibody–drug conjugates (ADCs), bispecific mAbs that recognize 2 different targets, fusion mAbs such as immunocytokines and mAb fragments. Introduction of all these smart targeted molecules is accompanied by questions about their behavior and biodistribution in the human body. The term *immuno-PET* is also used for tracking of other slow-kinetic targeting vehicles such as therapeutic cells (e.g., stem cells and immune cells) and nanoparticles.

During the past decade, ^{89}Zr-immuno-PET has been recognized by academic and pharma research centers as a powerful tool in drug development and precision medicine, both preclinically and clinically, for a variety of in vivo purposes: assessment of target expression; evaluation of the behavior of the drug in relation to its intrinsic properties and optimization of drug design; optimization of the dose, route, and schedule of administration (intravenous); prediction of the efficacy and toxicity of drug treatment by performing target occupancy studies; and selection of patients with the highest chance of benefit from drug treatment (*7*).

In this review, after summarizing the most important technical aspects of ^{89}Zr-immuno-PET, we use appealing showcases to illustrate the current potential of ^{89}Zr-immuno-PET in the characterization of novel therapeutic biologic drugs and their targets. The review is not intended to be comprehensive with respect to PET imaging in drug development; for a more comprehensive review, we refer the reader to previous publications (*8–10*).

TECHNICAL STATE OF THE ART OF ^{89}ZR-IMMUNO-PET

^{89}Zr-Labeled Tracer Production

To enable the visualization and quantification of a targeted drug with a PET camera, the drug should be labeled in an inert way with a positron-emitting radionuclide. Moreover, the physical half-life of the positron emitter should be compatible with the residence time of the drug in the body, which is typically several days to weeks for long-circulating intact mAbs of 150 kDa. This makes the positron emitter ^{89}Zr, with its half-life of 78.4 h, a preferred isotope also with regard to ease of transportation and logistics. In addition, ^{89}Zr is a residualizing isotope that becomes trapped inside the cell after internalization by the mAb, and its physical characteristics are well suited for high-resolution and quantitative PET imaging.

^{89}Zr can be produced efficiently by irradiation of natural yttrium with 13-MeV protons (^{89}Y(p,n)^{89}Zr nuclear reaction). Several academic and commercial suppliers make ^{89}Zr available worldwide on a daily base.

For stable coupling of ^{89}Zr to targeting ligands such as mAbs, a chelator has to be used. Currently, most ^{89}Zr-immuno-PET studies use desferrioxamine B (DFO). The conjugation procedures most often apply either the 2,3,5,6-tetrafluorophenol activated ester of *N*-succinyl-DFO-Fe (2,3,5,6-tetrafluorophenol-*N*-suc-DFO-Fe, in which DFO is protected by Fe^{3+}) or the *p*-isothiocyanatobenzyl-DFO, forming, respectively, stable amide or thiourea bonds with lysine residues in proteins. Both chelators are commercially available, and detailed conjugation and labeling protocols for the current-good-manufacturing-practice–compliant production of ^{89}Zr-labeled mAbs have been published for both (*11,12*). Although radiolabeling is performed mostly manually, protocols for fully automated current-good-manufacturing-practice–compliant production of ^{89}Zr-labeled mAbs on a commercially available synthesis module have been described (*13*). Although several modifications of these protocols have been proposed to extend the applicability of ^{89}Zr-immuno-PET, such as by providing various options for random as well as site-specific conjugation, the basic principles have not been changed over the years (*14,15*). Nevertheless, it appeared from preclinical studies that the ^{89}Zr-DFO complex is prone to dissociation in vivo, resulting in free ^{89}Zr that accumulates in bone tissue. Many efforts have been invested to develop chelators with increased in vivo stability. From an inorganic chemistry perspective, DFO is not the ideal coordinating molecule for ^{89}Zr, because DFO is a hexadentate chelator consisting of 3 hydroxamate moieties whereas Zr^{4+} prefers forming octadentate complexes. Therefore, at least 15 new chelators have been proposed recently (*14,16*). When comparing the performance of these chelators, it appears that the octadentate analog of DFO consisting of 4 hydroxamate moieties, called DFO* ("DFO star"), is able to solve the instability issues observed with ^{89}Zr-DFO (Fig. 1) (*17*). Because the bifunctional variant DFO*-NCS is now commercially available, its translation to the clinic can be expected soon.

Several papers have described the quality controls that are needed to manufacture ^{89}Zr-labeled products according to current good manufacturing practices for clinical use (*11,12*). By following such an approach, the extrapolation can be made that the properties of the ^{89}Zr-labeled drug do not deviate from those of the parental drug. Since extensive data revealed the clinical safety of the DFO-based chelators, it can be justified that toxicology studies performed with the parental drug (for human use) are sufficient to also allow clinical use of the ^{89}Zr-labeled drug. The regulatory agencies of several European countries and of the United States have adopted this policy, which eases the integration of ^{89}Zr-immuno-PET into clinical research.

^{89}Zr-Tracer Quantification

PET has the intrinsic potential to quantify the uptake of ^{89}Zr-labeled drugs in diseased areas and normal organs. Makris et al. have addressed the accuracy of quantification by providing ^{89}Zr scanning procedures, which, independently of the scanner type or vendor, result in harmonized image quality (*18*). For this purpose, in addition to scanner cross-calibration, image noise and recovery coefficients also have to be aligned. Standardization of the

NOTEWORTHY

- ^{89}Zr-immuno-PET has become an important tool for the in vivo visualization and quantification of biologic drugs and the validation of disease targets.
- High-quality ^{89}Zr, suitable chelators for coupling, and standardized protocols for current-good-manufacturing-practice–compliant manufacturing of ^{89}Zr-labeled biopharmaceuticals are available.
- ^{89}Zr-immuno-PET is used for imaging of not only antibodies but also other slow-kinetic drugs, living therapeutic cells included.
- ^{89}Zr-immuno-PET has been adopted by academia as well as by the pharma industry.

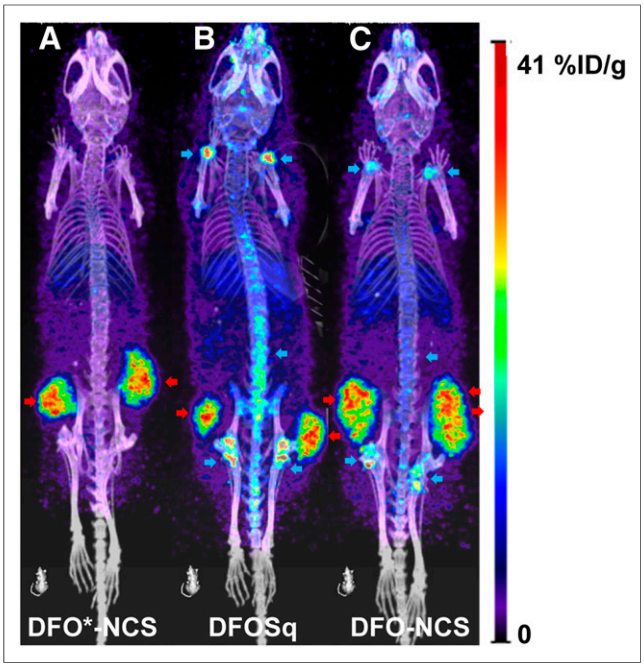

FIGURE 1. PET images of N87 tumor–bearing mice injected with ^{89}Zr-DFO*-NCS-trastuzumab (A), ^{89}Zr-DFO-squaramide-trastuzumab (B), or ^{89}Zr-DFO-NCS-trastuzumab (C) and scanned 144 h after injection. Tumors are indicated with red arrows and bone uptake with blue arrows. Bone uptake seen with the 2 DFO chelators is lacking when DFO* is used for ^{89}Zr labeling (*17*). %ID/g = percentage injected dose per gram.

quantification of ^{89}Zr-labeled compounds will enhance the potential impact of immuno-PET and facilitate evaluation in multicenter trials.

Drug uptake can be expressed as SUV or percentage injected dose per gram of tissue. Although it might seem attractive to relate mAb uptake to, for example, target antigen expression, efficacy, and toxicity, it is important to realize that total tissue uptake is the sum of target-specific contribution (i.e., specific uptake) and nonspecific uptake. Nonspecific uptake can be reversible (e.g., blood volume) or irreversible (due to ^{89}Zr-residualization after mAb uptake and degradation by antigen-negative cells). Jauw et al. recently described the nonspecific uptake of mAbs in normal tissues without known target expression by using quantitative ^{89}Zr-immuno-PET at multiple time points (*19*). These results form a crucial basis for determination of target occupancy, that is, the target-specific drug uptake. Although the nonspecific contribution might be relatively constant for normal tissues across patients, this most probably will not be the case for tumors and therefore more sophisticated modeling strategies have to be developed.

The level of target-specific mAb uptake as measured with ^{89}Zr-immuno-PET might depend on the mAb dose used and can lead to erroneous interpretations with respect to the tumor-targeting potential of the drug. When the mAb dose is too high, target saturation might occur, resulting in low tumor-to-nontumor ratios and poor delineation of tumors on PET images. However, poor tumor targeting on PET might also be the result of a mAb dose that is too low, such as when there is a high level of target antigen expression in easily accessible normal organs (antigen sink) or when there is soluble (shed) target antigen present in the blood circulation. Since tumor target engagement and the identification of potential antigen sinks are informative in the in vivo characterization of novel candidate mAb–target combinations, it is recommended that ^{89}Zr-immuno-PET (pharmacokinetics included) be applied in mAb dose escalation studies.

Also, technical advancements such as the introduction of total-body PET/CT scanners, having unprecedented sensitivity and high spatial resolution, will likely facilitate assessment of target engagement. As shown recently, the combination of total-body PET and highly stable DFO* chelators enables meaningful ^{89}Zr-antibody PET studies at up to 30 d after injection (*20*). At such late time points, it can be anticipated that ^{89}Zr tissue uptake is dominated by the target-specific contribution whereas the blood-pool contribution will be negligible. However, wide introduction of total-body PET/CT systems may be hampered by their high costs and limited availability. Therefore, good yet less optimal alternatives are the recently introduced digital PET/CT systems with an axial field of view of about 20 cm or more. These digital systems have excellent sensitivities and improved time-of-flight performance compared with current analog systems, and these systems already show improved image quality or provide opportunities to lower injected activities, thereby reducing radiation burden (*21*). Most studies with intact mAbs use 37–74 MBq of ^{89}Zr and result in an effective radiation dose of 20–40 mSv (*22*). This is justified for cancer patients but not for nononcologic patients, for whom the dose limit in Europe is 10 mSv. Since total-body PET/CT is 20–40 times more sensitive—and digital systems about 3 times more sensitive—for total-body imaging than is conventional PET/CT, this opens opportunities for using less radioactivity, late imaging time points, repeated tracer administration, imaging in diseased as well as healthy subjects, imaging in adults and children, and combinations of these.

^{89}ZR-IMMUNO-PET IN DRUG DEVELOPMENT

^{89}Zr-immuno-PET can be used for the in vivo validation of targeting compounds and disease targets. To this end, the in vivo biodistribution of biologic drugs, including target occupancy, can be studied in relation to drug characteristics such as specificity, affinity, size, dose, functional modifications, and physicochemical properties in general; target or antigen expression, modulation, and internalization; and route of administration. On the basis of the biodistribution findings, strategies can be explored to further improve target engagement, drug delivery, and drug potency with the aim of widening the therapeutic window. The next section discusses some appealing examples in which ^{89}Zr-immuno-PET is used to characterize key features of biologicals.

mAbs

Most of the ^{89}Zr-immuno-PET studies have been performed with conventional FDA-approved intact mAbs, directed against well-characterized antigens expressed on cancer lesions. Therefore, these studies are focusing on response prediction and patient selection rather than on drug or target selection (*23*). In addition to these approved mAbs, more recently several other ^{89}Zr-labeled biopharmaceuticals entered clinical trials, as comprehensively shown by Supplemental Table 1, which includes related publications (supplemental materials are available at http://jnm.snmjournals.org).

Trastuzumab, directed against human epidermal growth factor receptor 2 (HER2), has been most intensively studied (*23*). In a first clinical study, ^{89}Zr-immuno-PET was applied in 14 patients for imaging of HER2-positive metastatic breast cancer lesions (*24*). ^{89}Zr-trastuzumab was used at a dose of 10 or 50 mg for

those patients who were trastuzumab-naïve and 10 mg for those who were already on trastuzumab treatment. Figure 2 clearly illustrates the dose-dependent biodistribution of ^{89}Zr-trastuzumab. The 10-mg trastuzumab dose resulted in a relatively high uptake in the liver and a pronounced intestinal excretion of ^{89}Zr-trastuzumab, which can be explained by low levels of circulating HER2 in the blood (antigen sink) causing complex formation and excretion via the liver. However, with the 50-mg dose, ^{89}Zr-immuno-PET revealed uptake of trastuzumab in most of the known lesions, brain metastases included, and in previously undetected lesions (Fig. 3). No evidence for HER2 expression in normal organs was found, as was confirmed by quantitative PET analysis (*19*). These results indicate that the drug–target combination trastuzumab–HER2 shows ideal properties for selective tumor targeting and therefore justifies the development of more potent anti-HER2 therapeutics.

Targeting of HER2 is more tumor-selective than targeting of the ErbB receptor family members HER1 (i.e., EGFR, epidermal growth factor receptor) and HER3, as revealed from clinical trials with ^{89}Zr-labeled cetuximab (anti-EGFR) and the mAbs RG7116 (lumretuzumab) and GSK2849330, both directed against HER3 (*25–27*). With ^{89}Zr-cetuximab in addition to tumor targeting, increased liver uptake (≤23 percentage injected dose per gram of tissue) was also observed during the first days after injection (Fig. 4) (*25*). Although ^{89}Zr-immuno-PET images always show liver uptake due to normal mAb catabolism, in the case of ^{89}Zr-cetuximab the liver uptake appeared much higher and can be explained by physiologic EGFR expression (*19*). Increased liver and spleen uptake was also observed with the 2 mentioned anti-HER3 mAbs (*26,27*). These results indicate that normal-tissue expression of EGFR and HER3 hampers efficient tumor targeting and might limit the use of potent drug formats directed against these targets.

Immune Checkpoint Inhibitors (ICIs)

Besides tumor cells, stromal cells such as immune cells or fibroblasts also are exploited as target cells for therapy with biologicals. ICIs, which can block immune inhibitory checkpoints and, by doing so, boost T-cell–mediated antitumor response, have been proven to be particularly successful. Therapy with approved mAbs targeting cytotoxic T-lymphocyte–associated antigen (anti-CTLA4: ipilimumab), programmed cell death protein 1 (anti-PD-1: nivolumab, pembrolizumab, and cemiplimab), and programmed death ligand 1 (anti-PD-L1: atezolizumab, avelumab, and durvalumab) results in durable responses in various tumor types. The list of biologicals, targets, and indications for ICI therapy is steadily growing. Despite this progress, just a small portion of eligible patients responds to ICI therapy, and this raises the question: why? (*28*). These exciting developments have boosted the exploration of imaging biomarkers for ICI therapy (*29*). Although clinical imaging of ICIs is at an early stage, 2 trials have been reported. In one study, PET with ^{89}Zr-atezolizumab (PD-L1) was performed on 22 patients before atezolizumab treatment (*30*). Tumor uptake of ^{89}Zr-atezolizumab positively correlated with a response to atezolizumab treatment when immunohistochemistry failed to predict a treatment response. In addition, high uptake of ^{89}Zr-atezolizumab was found in healthy lymphoid tissues, including spleen, lymph node, and Waldeyer ring, raising the question of whether such uptake might be responsible for immune-related adverse events. In another study, ^{89}Zr-nivolumab (PD-1) and an ^{18}F-labeled anti-PD-L1 adnectin protein (^{18}F-BMS-986192) were both evaluated in 13 non–small cell lung cancer patients before nivolumab treatment (*31*). It is assumed that high PD-L1 expression by tumor cells, together with high PD-1 expression by tumor-infiltrating lymphocytes, is a favorable condition for response to anti-PD1/PD-L1 ICI therapy. In this study, tumor uptake of both tracers correlated with PD1 and PD-L1 expression as assessed by immunohistochemistry in tumor tissue, as illustrated by Figure 5. For both tracers, a higher tumor uptake was found in responding tumors than in nonresponding tumors; however, this predictive value needs to be confirmed in larger patient cohorts.

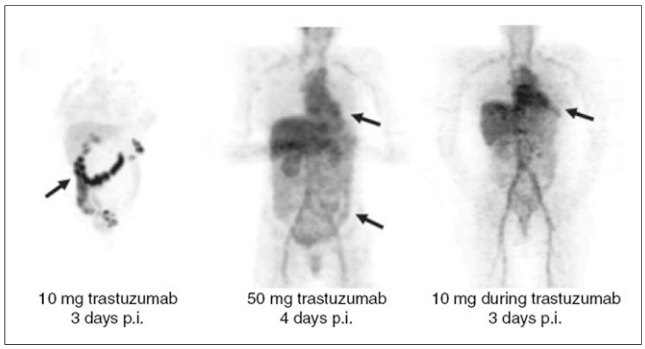

FIGURE 2. Dose-dependent ^{89}Zr-trastuzumab biodistribution. Radioactivity in blood pool and intestinal excretion is indicated by arrows. Trastuzumab clears rapidly from body at low mAb dose (*24*). p.i. = after injection.

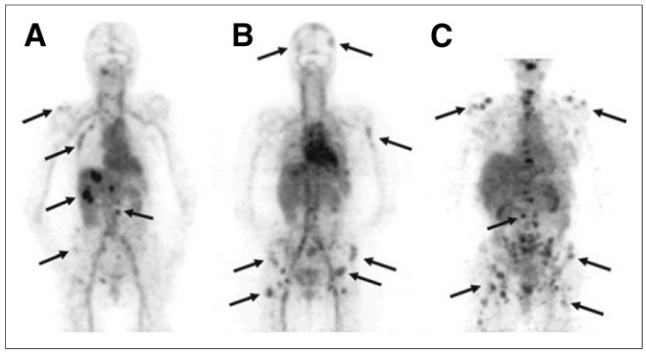

FIGURE 3. Examples of ^{89}Zr-trastuzumab uptake 5 d after injection in patient with liver and bone metastases (A) and in 2 patients with multiple bone metastases (B and C). Several lesions have been indicated by arrows (*24*).

ADCs

ADCs are the Trojan horses of antibody development: they represent a targeted approach to treating cancer, allowing selective delivery of therapeutic drugs (payloads) to the malignant cells by mAbs and thus avoiding damage to healthy cells. Currently, 9 ADCs are approved by the FDA and more than 100 are under clinical evaluation (*32*). ADCs comprise 3 components: a disease-selective mAb, a highly potent small-molecule therapeutic payload, and a linker that connects the 2 parts. Ideally, the ADC is fully stable in the circulation and selectively accumulates to a high extent and homogeneously in the tumor, where it is internalized and the drug is released to exerts its toxic effects. Despite the growing interest, several ADCs failed very recently, mostly because of insufficient efficacy or unforeseen toxicities (*32,33*). Toxicities can be due to the unfavorable selectivity or specificity of the antibody, as has occurred

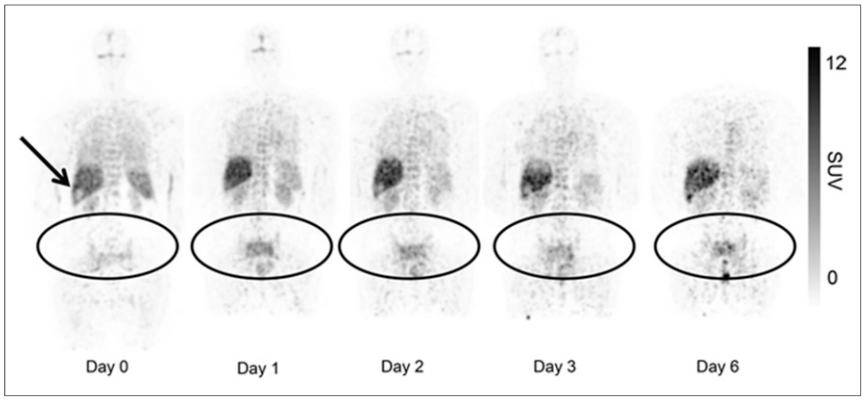

FIGURE 4. Uptake of ^{89}Zr-cetuximab in patient with tumor lesions in pelvis and sacral bone. ^{89}Zr-cetuximab is sequestered in liver, and relatively photopenic lesion is observed at site of liver metastasis (arrow). Accumulation of ^{89}Zr-cetuximab over time is demonstrated in tumor lesions (*25*).

with ADCs based on anti-EGFR antibodies. Still, toxicity can also be related to the instability of the linker system or the poor solubility of the drug used. First, the drug can be released from the mAb in the circulation, resulting in sequestration of the drug in normal tissues. Second, the mAb can be destabilized by drug conjugation, resulting in faster blood clearance of the ADC and sequestration in catabolic organs such as liver and spleen. Destabilization occurs when the drug-to-mAb ratio is too high, especially when the drug is hydrophobic. Third, after uptake of an ADC by the tumor cell and subsequent catabolism, the drug can be detached from the ADC and eventually be released from the cell, enter the circulation, and cause toxicity. Trends and challenges in ADC development have been described in a recent review (*33*).

Several ^{89}Zr-immuno-PET studies have been performed to support the development and application of ADCs. Most of these studies have been performed with the radiolabeled parental antibody and not with the radiolabeled ADC (*34–38*). The use of radiolabeled parental mAb for imaging might be informative to assess tumor selectivity and target occupancy and to predict the efficacy of ADC treatment (*37,38*). Related to this, it is not surprising that HER2 has been recognized as an ideal target for ADC approaches. In fact, 2 anti-HER2 ADCs have been FDA-approved for treatment of metastatic breast cancer, ado-trastuzumab emtansine (Kadcyla, T-DM1; Genentech) and trastuzumab deruxtecan (Enhertu, DS-8201; Daiichi Sankyo Co., Ltd.), and several others are under development (*32*). Because drug loading might affect the biodistribution of a mAb, ^{89}Zr-immuno-PET is most informative when the ADC itself (carrier + cargo) is radiolabeled rather than just the parental antibody (carrier), as has been explored in some preclinical studies (*39–43*).

For the in vivo evaluation of ADCs, it is important to learn from the biodistribution of both the mAb and the therapeutic payload. Cohen et al. used dual radiolabeling by covalently coupling ^{131}I-labeled tubulysin analogs as therapeutic payload to ^{89}Zr-labeled trastuzumab, resulting in ^{131}I-tubulysin-^{89}Zr-trastuzumab ADCs (*41*). By doing so, the stability of the ADCs could easily be demonstrated in vitro as well as in vivo. Moreover, it could be concluded that coupling of the tubulysin analogs did not alter the pharmacokinetics and tumor-targeting properties of trastuzumab (inert coupling).

In their effort to characterize the in vivo stability of a novel ADC linker—the platinum-based linker (ethylenediamine)platinum(II)$^{2+}$ (called *Lx*; LinXis Biopharmaceuticals)—Muns et al. labeled the mAb with ^{89}Zr, labeled the *Lx* linker with ^{195m}Pt (γ-emitter with a half-life time of 4.02 d), and exploited ^{89}Zr-DFO as an artificial payload (*42*). A similar biodistribution was observed irrespective of the isotope measured, which led to the conclusion that *Lx*-based ADCs are fully stable in vitro and in vivo and capable of optimal delivery of the artificial payload to tumors. In a next step, the commonly used therapeutic payload auristatin F was coupled at various molar ratios to trastuzumab via the *Lx* linker followed by ^{89}Zr labeling to obtain ^{89}Zr-DFO-trastuzumab-*Lx*-auristatin F with auristatin F–to–antibody ratios of 0, 2.6, or 5.2. (Fig. 6). Although ADCs with a drug-to-mAb ratio of 2.6 showed the same selective tumor targeting as the parental antibody (indicated as a drug-to-mAb ratio of 0), the ADC with a drug-to-mAb ratio of 5.2 showed dramatically impaired tumor targeting, faster blood clearance, and increased liver uptake. After validation of optimal tumor targeting by imaging, the trastuzumab-*Lx*-auristatin F ADC appeared to outperform FDA-approved

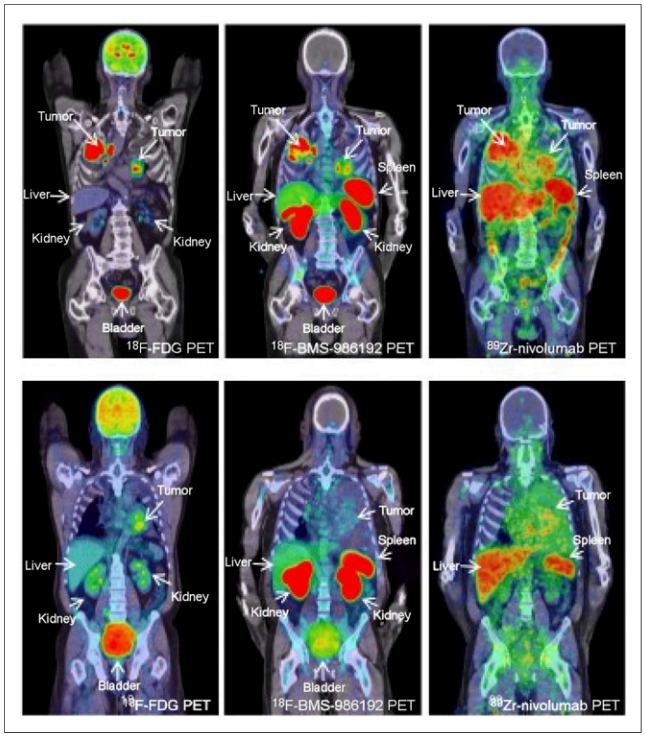

FIGURE 5. PET images of 2 NSCLC patients. (Top) Patient with PD-L1 expression in 95% of tumor cells. (Bottom) Patient with tumor PD-L1 expression of <1%. ^{18}F-FDG PET (left) demonstrates high glucose metabolism of tumors in both lungs and mediastinal lymph nodes; ^{18}F-BMS-986192 PD-L1 PET (middle) and ^{89}Zr-labeled nivolumab PD-1 PET (right) demonstrate high but heterogeneous tracer uptake in tumors of top patient and low heterogeneous tracer uptake in tumor of bottom patient (*31*).

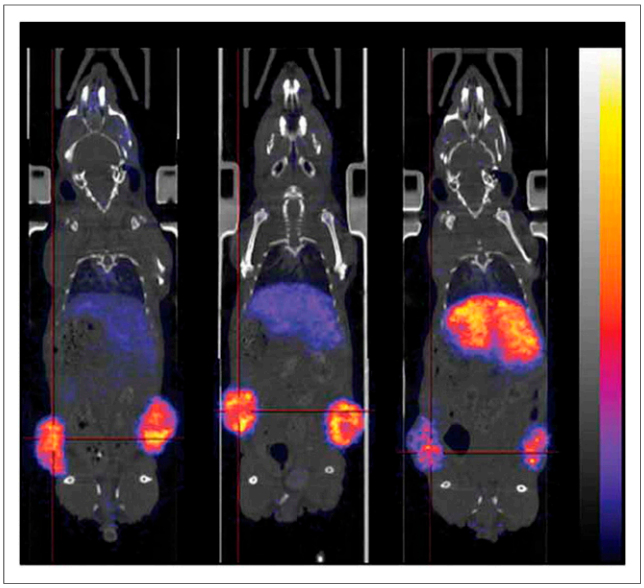

FIGURE 6. Effect of auristatin F (AF) conjugation via *Lx* linker to trastuzumab on biodistribution characteristics in NCI-N87–bearing nude mice. Shown are PET images of ^{89}Zr-trastuzumab-*Lx*-auristatin F with auristatin F–to–mAb ratios of 0 (left), 2.6 (middle), and 5.2 (right) 96 h after injection. Tumor targeting is impaired and liver uptake increased for ADC with auristatin F–to–mAb ratio of 5.2 (*43*).

ado-trastuzumab emtansine in therapy studies on tumor-bearing mice (*43*).

Activatable Antibodies

Unfortunately, only a limited number of target antigens have high expression on tumor or diseased tissue and very low expression on healthy tissue. Activatable antibodies, such as those under development by CytomX Therapeutics (so-called Probody therapeutics), represent a potential new approach for improving the selectivity and homogeneity of tumor targeting by antibodies. This approach aims to widen the therapeutic window and increase the number of candidate targets that are suitable for targeting with potent antibody constructs such as ADCs. Activatable antibodies are recombinant antibody prodrugs in which the antigen-binding domains are masked and converted to active antigen-binding antibodies inside the tumor environment by tumor-associated proteases (Fig. 7). The first in vivo proof of concept was obtained with an anti-EGFR Probody therapeutic based on the anti-EGFR mAb cetuximab (*44*). In these studies, it was demonstrated that the Probody remained masked until activated by proteases in the tumor environment, a way to circumvent accumulation of cetuximab in normal tissues (e.g., liver and skin). Two Probody therapeutic candidates have been evaluated in preclinical ^{89}Zr-immuno-PET studies.

In one study, the tumor-targeting performance of the anti-CD166 Probody–drug conjugate CX-2009, a Probody therapeutic coupled with the toxic drug DM4, was labeled with ^{89}Zr and evaluated with PET in xenograft-bearing mice (*45*). CD166 is overexpressed on the outer cell surface of many tumor types but is also present in several healthy organs. In this study, the biodistribution of CX-2009 was compared with the biodistribution of the Probody therapeutic itself (without drug), the parental mAb (no mask), and the parental mAb coupled with DM4 (ADC). These studies demonstrated that CX-2009 is capable of optimally targeting CD166-expressing tumors when compared with its parental compounds, implying that enzymatic activation inside the tumor, required for CD166 binding, does not limit tumor targeting. Reduced targeting of healthy organs cannot be demonstrated in rodents because CX-2009 does not bind to mouse CD166; however, ongoing clinical ^{89}Zr-immuno-PET studies should provide confirmation.

In another preclinical study, it was demonstrated that the anti-PD-L1 Probody CX-072 therapeutic became activated in tumors, resulting in preferential tumor uptake, whereas accumulation in spleen and other PD-L1–expressing peripheral lymphoid organs appeared to be limited (*46*). These results indicate that CX-072 may reduce anti-PD-L1–mediated toxicity in healthy tissues. These intriguing findings will be confirmed in ongoing clinical ^{89}Zr-CX-072 studies.

Bispecific Antibodies (BsAbs) and Immunocytokines

Currently, more than 90 BsAbs have been developed, mostly for oncologic applications (*47*). Since such constructs contain 2 (or more) antigen-binding regions directed against 2 different targets, their biodistribution is hard to predict and will depend on, among other things, the expression level and accessibility of each of the targets and the affinity of each antibody arm for its particular antigen. Appropriate targeting, which means simultaneous binding to both targets, is certainly possible for hematooncologic applications such as in the case of the FDA-approved anti-CD3-CD19 BsAb blinatumomab, because here the CD3+ cytotoxic T cells (effector cells) and the CD19+ B cells (target cells) are residing in the same blood compartment. However, appropriate targeting will theoretically be much more challenging in the case of solid tumors. For example, an anti-CD3-HER2 BsAb that is administered intravenously will most likely show impaired tumor targeting, since the anti-CD3 arm will cause stickiness of the BsAb to T cells in the blood compartment. A few clinical ^{89}Zr-immuno-PET studies indicate that that indeed seems to be the case.

Moek et al. evaluated a 55-kDa ^{89}Zr-labeled BsAb directed against CD3 and the carcinoembryonic antigen (CEA) in 9 patients with advanced gastrointestinal adenocarcinomas (*48*). The tracer was administered either at a low dose of 0.2, 2, or 5 mg of BsAb or during a treatment period in which the patients received 6.4 or 12.8 mg of BsAb/d by continuous intravenous administration via a central venous access port. As might have been expected, images with the tracer dose revealed accumulation of ^{89}Zr-labeled anti-CD3-CEA BsAb in CD3-rich lymphoid organs, as well as inter- and intraindividual heterogenous tumor uptake. Interestingly, tracer

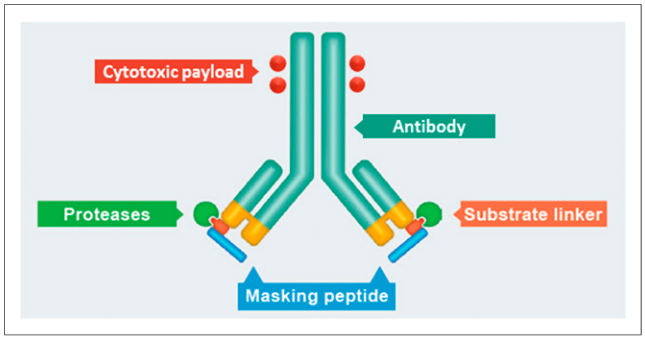

FIGURE 7. General representation and structure of CX-2009 Probody drug conjugate. (Courtesy of CytomX Therapeutics, Inc.)

administration during BsAb treatment revealed the presence of the tracer in the blood pool, whereas tumor lesions were not visualized, possibly reflecting target saturation. These studies indicate that target saturation in the tumor might be possible, although at the expense of using an inconvenient administration procedure. To improve tumor targeting and to avoid on-target, off-tumor toxicity, several novel BsAb constructs are under development, including BsAbs comprising a masked CD3 arm—BsAbs that need activation inside the tumor to exert their bispecific activity (*49*).

Similar observations have been made for the immunocytokine cergutuzumab amunaleukin, an immunocytokine directed against CEA with abolished IL-2α receptor binding, which is designed to cause intratumoral interleukin-2 (IL-2)–mediated immune potentiation (*50*). Besides improved uptake in CEA-positive tumors when compared with CEA-negative tumors, major accumulation in lymphoid organs was also observed, as is compatible with binding to immune cells expressing the IL-2 receptor.

Other Emerging Fields of ^{89}Zr-Immuno-PET

Cell-based therapies such as adoptive immunotherapy (e.g., chimeric antigen receptor T cells) and stem cell therapy have received considerable attention (*51*). Also here, ^{89}Zr-immuno-PET might be informative to assess the in vivo distribution of the therapeutic cell population (*52*). Besides identifying immune cell subsets with ^{89}Zr-labeled PET tracers based on their specific cell-surface markers, adoptive cells today can also be uploaded with ^{89}Zr via ^{89}Zr-oxine or covalently membrane-labeled with ^{89}Zr via DFO, to enable their tracking in vivo (*53*). For this purpose, cells have to be labeled with sufficient amounts of ^{89}Zr, and this labeling must be done inertly, that is, without affecting the cells' biologic properties. Although cell tracking with ^{89}Zr-immuno-PET is at a pioneering stage, even the possibility of single-cell tracking by PET has recently been demonstrated in mice (*54*).

In addition to drug and target characteristics, the route of administration might also be an important variable in the efficient application of biopharmaceuticals, as was illustrated in a couple of ^{89}Zr-immuno-PET studies on brain targeting. One of these studies was the first to apply ^{89}Zr-bevacizumab PET imaging in pediatric patients with diffuse intrinsic pontine glioma, demonstrating low and variable ^{89}Zr-bevacizumab tumor uptake after intravenous administration (*55*). These findings indicate the added value of ^{89}Zr-immuno-PET in explaining the poor prognosis of these patients by blood–brain barrier integrity. Interestingly, in subsequent preclinical PET studies with ^{89}Zr-bevacizumab, Lesniak et al. showed that by intraarterial instead of intravenous administration of the conjugate and coadministration of mannitol for opening of the blood–brain barrier, the brain uptake of ^{89}Zr-bevacizumab became 10–15 times higher (*56*). These studies illustrate that ^{89}Zr-immuno-PET could guide delivery of biologicals behind the blood–brain barrier, with great promise for therapy of brain diseases, neurodegenerative diseases included (*57*).

CONCLUSION

The field of ^{89}Zr-immuno-PET is expanding rapidly, as exemplified by the increasing number of publications, the types of applications and biopharmaceuticals under study, and the number of clinical trials. As illustrated in this review, ^{89}Zr-immuno-PET has become an important tool for the in vivo characterization of biologic drugs and the validation of disease targets. Although ^{89}Zr-labeling of biopharmaceuticals seems to be technically matured and can for most drug formats be performed in an inert and pharmaceutically acceptable way, improvements in ^{89}Zr-immuno-PET can be expected in the coming years by standardization and harmonization of ^{89}Zr quantification by PET imaging and by the introduction of more sensitive PET scanners. In an era of societal debate about expensive drugs and the affordability of health care, ^{89}Zr-immuno-PET might become a crucial player in improving the efficiency and effectiveness of drug development and in the further evolution of precision medicine.

DISCLOSURE

Guus van Dongen has the unpaid position of chief scientific officer at LinXis Biopharmaceuticals. No other potential conflict of interest relevant to this article was reported.

REFERENCES

1. Paul SM, Mytelka DS, Dunwiddie CT, et al. How to improve R&D productivity: the pharmaceutical industry's grand challenge. *Nat Rev Drug Discov.* 2010;9: 203–214.
2. Baedecker M, Ringel M, Schulze U. 2018 FDA approvals hit all time high—but average value slips again. *Nat Rev Drug Discov.* 2019;18:90.
3. Walsh G. Biopharmaceutical benchmarks 2018. *Nat Biotechnol.* 2018;36:1136–1145.
4. Kaplon H, Reichert JM. Antibodies to watch in 2019. *MAbs.* 2019;11:219–238.
5. Pammolli F, Righetto L, Abrignani S, Pani L, Pelicci PG, Rabosio E. The endless frontier? The recent increase of R&D productivity in pharmaceuticals. *J Transl Med.* 2020;18:162.
6. Börjesson PKE, Jauw YWS, Boellaard R, et al. Performance of immuno-positron emission tomography with zirconium-89-labeled chimeric monoclonal antibody U36 in the detection of lymph node metastases in head and neck cancer patients. *Clin Cancer Res.* 2006;12:2133–2140.
7. Jauw YW, Menke-van der Houven van Oordt CW, Hoekstra OS, et al. Immuno-positron emission tomography with zirconium-89-labeled monoclonal antibodies in oncology: what can we learn from initial clinical trials? *Front Pharmacol.* 2016;7:131.
8. Kelloff GJ, Krohn KA, Larson SM, et al. The progress and promise of molecular imaging probes in oncologic drug development. *Clin Cancer Res.* 2005;11:7967–7985.
9. de Vries EG, Kist de Ruijter L, Lub-de Hooge MN, Dierckx RA, Elias SC, Oosting SF. Integrating molecular nuclear imaging in clinical research to improve cancer therapy. *Nat Rev Clin Oncol.* 2019;16:241–255.
10. Wei W, Rosenkrans ZT, Liu J, Huang G, Luo Q-Y, Cai W. ImmunoPET: concept, design and applications. *Chem Rev.* 2020;120:3787–3851.
11. Vosjan MJWD, Perk LR, Visser GWM, et al. Conjugation and radiolabeling of monoclonal antibodies with zirconium-89 for PET imaging using the bifunctional chelate *p*-isothiocyanatobenzyl-desferrioxamine. *Nat Protoc.* 2010;5:739–743.
12. Cohen R, Vugts DJ, Stigter-van Walsum M, Visser GWM, Van Dongen GAMS. Inert coupling of IRDye800CW and zirconium-89 to monoclonal antibodies for single- or dual-modal fluorescence and PET imaging. *Nat Protoc.* 2013;8:1010–1018.
13. Poot AJ, Adamzek KWA, Windhorst AD, et al. Fully automated ^{89}Zr labeling and purification of antibodies. *J Nucl Med.* 2019;60:691–695.
14. Heskamp S, Raavé R, Boerman O, Rijpkema M, Goncalves V, Denat F. ^{89}Zr-immuno-positron emission tomography in oncology: state-of-the-art ^{89}Zr radiochemistry. *Bioconjug Chem.* 2017;28:2211–2223.
15. Bhatt NB, Pandya DN, Rideout-Danner S, Gage HD, Marini FC, Waddas TJ. A comprehensively revised strategy that improves the specific activity and long-term stability of clinically relevant ^{89}Zr-immuno-PET agents. *Dalton Trans.* 2018;47: 13214–13221.
16. Bhatt NB, Pandya DN, Wadas TJ. Recent developments in zirconium-89 chelator development. *Molecules.* 2018;23:638.
17. Chomet M, Schreurs M, Bolijn MJ, et al. Head to head comparison of DFO* and DFO chelators: selection of the best candidate for clinical ^{89}Zr-immuno-PET. *Eur J Nucl Med Mol Imaging.* September 5, 2020 [Epub ahead of print].
18. Makris NE, Boellaard R, Visser EP, et al. Multicenter harmonization of ^{89}Zr PET/CT performance. *J Nucl Med.* 2014;55:264–267.
19. Jauw YWS, O'Donoghue JA, Zijlstra JM, et al. ^{89}Zr-immuno-PET: towards a non-invasive clinical tool to measure target engagement of therapeutic antibodies in vivo. *J Nucl Med.* 2019;60:1825–1832.

20. Berg E, Gill H, Marik J, et al. Total-body PET and highly stable chelators together enable meaningful ^{89}Zr-antibody-PET studies up to 30 days post-injection. *J Nucl Med.* 2020;61:453–460.
21. van Sluis J, Boellaard R, Somasundaram A, et al. Image quality and semiquantitative measurements on the Biograph Vision PET/CT system: initial experiences and comparison with the Biograph mCT. *J Nucl Med.* 2020;61:129–135.
22. Börjesson PK, Jauw YWS, De Bree R, et al. Radiation dosimetry of ^{89}Zr-labeled chimeric monoclonal antibody U36 as used for immuno-PET in head and neck cancer patients. *J Nucl Med.* 2009;50:1828–1836.
23. Yoon J-K, Park B-N, Ryu E-K, An Y-S, Lee S-J. Current perspectives on ^{89}Zr-PET imaging. *Int J Mol Sci.* 2020;21:4309.
24. Dijkers EC, Oude Munnink TH, Kosterink JG, et al. Biodistribution of ^{89}Zr-trastuzumab and PET imaging of HER2-positive lesions in patients with metastatic breast cancer. *Clin Pharmacol Ther.* 2010;87:586–592.
25. Menke-van der Houven van Oordt CW, Gootjes EC, Huisman MC, et al. ^{89}Zr-cetuximab PET imaging in patients with advanced colorectal cancer. *Oncotarget.* 2015;6:30384–30393.
26. Bensch F, Lamberts LE, Smeenk MM, et al. ^{89}Zr-lumretuzumab PET imaging before and during HER3 antibody lumretuzumab treatment in patients with solid tumors. *Clin Cancer Res.* 2017;23:6128–6137.
27. Menke-van der Houven van Oordt CW, McGeoch A, Bergstrom M, et al. Immuno-PET imaging to assess target engagement: experience from ^{89}Zr-anti-HER3 mAb (GSK2849330) in patients with solid tumors. *J Nucl Med.* 2019;60:902–909.
28. Haslam A, Prasad V. Estimation of the percentage of US patients with cancer who are eligible for and respond to checkpoint inhibitor immunotherapy drugs. *JAMA Netw Open.* 2019;2:e192535.
29. van de Donk PP, Kist de Ruijter L, Lub-de Hooge MN, et al. Molecular-imaging biomarkers for immune-checkpoint inhibitor therapy. *Theranostics.* 2020;10:1708–1718.
30. Bensch F, Van der Veen EL, Lub-de Hooge MN, et al. ^{89}Zr-atezolizumab imaging as a non-invasive approach to assess clinical response to PD-L1 blockade in cancer. *Nat Med.* 2018;24:1852–1858.
31. Niemeijer AN, Leung D, Huisman MC, et al. Whole body PD-1 and PD-L1 positron emission tomography in patients with non-small-cell lung cancer. *Nat Commun.* 2018;9:4664.
32. Joubert N, Beck A, Dumontet C, Denevault-Sabourin C. Antibody-drug conjugates: the last decade. *Pharmaceuticals (Basel).* 2020;13:245.
33. Beck A, Goetsch L, Dumontet C, Corvaïa N. Strategies and challenges for the next generation of antibody-drug conjugates. *Nat Rev Drug Discov.* 2017;16:315–337.
34. Carmon KS, Azhdarinia A. Application of immuno-PET in antibody-drug conjugate development. *Mol Imaging.* 2018;17:1536012118801223.
35. O'Donoghue JA, Danila DC, Pandit-Taskar N, et al. Pharmacokinetics and biodistribution of a [^{89}Zr]Zr-DFO-MSTP2109A anti-STEAP1 antibody in metastatic castration-resistant prostate cancer patients. *Mol Pharm.* 2019;16:3083–3090.
36. Chia P-L, Parakh S, Tsao M-S, et al. Targeting and efficacy of novel mAb806-antibody-drug conjugates in malignant mesothelioma. *Pharmaceuticals (Basel).* 2020;13:289.
37. Gebhart G, Lamberts LE, Wimana Z, et al. Molecular imaging as a tool to investigate heterogeneity of advanced HER2-positive breast cancer and to predict patient outcome under trastuzumab emtansine (T-DM1): the ZEPHIR trial. *Ann Oncol.* 2016;27:619–624.
38. Williams S-P, Ogasawara A, Tinianow JN, et al. ImmunoPET helps predicting the efficacy of antibody-drug conjugates targeting TENB2 and STEAP1. *Oncotarget.* 2016;7:25103–25112.
39. Al-Saden N, Lam K, Chan C, Reilly RM. Positron-emission tomography of HER2-positive breast cancer xenografts in mice with ^{89}Zr-labeled trastuzumab-DM1: a comparison with ^{89}Zr-labeled trastuzumab. *Mol Pharm.* 2018;15:3383–3393.
40. Kang L, Jiang D, Ehlerding EB, et al. Noninvasive trafficking of brentuximab vedotin and PET imaging of CD30 in lung cancer murine models. *Mol Pharm.* 2018;15:1627–1634.
41. Cohen R, Vugts DJ, Visser GWM, et al. Development of novel ADCs: conjugation of tubulysin analogues of trastuzumab monitored by dual radiolabeling. *Cancer Res.* 2014;74:5700–5710.
42. Muns JA, Montserrat V, Houthoff H-J, et al. In vivo characterization of platinum(II)-based linker technology for the development of antibody-drug conjugates: taking advantage of dual labeling with ^{195m}Pt and ^{89}Zr. *J Nucl Med.* 2018;59:1146–1151.
43. Sijbrandi NJ, Merkul E, Muns JA, et al. A novel platinum(II)-based bifunctional ADC linker benchmarked using ^{89}Zr-desferal and auristatin F conjugated trastuzumab. *Cancer Res.* 2017;77:257–267.
44. Desnoyers LR, Vasiljeva O, Richardson JH, et al. Tumor-specific activation of an EGFR-targeted probody enhances therapeutic index. *Sci Transl Med.* 2013;5:207ra144.
45. Chomet M, Schreurs M, Nguyen M, et al. The tumor targeting performance of anti-CD166 Probody drug conjugate CX-2009 and its parental derivatives as monitored by ^{89}Zr-immuno-PET in xenograft bearing mice. *Theranostics.* 2020;10:5815–5828.
46. Giesen D, Broer LN, Lub-de Hooge M, et al. Probody therapeutic design of ^{89}Zr-CX-072 promotes accumulation in PD-L1 expressing tumors compared to normal murine lymphoid tissue. *Clin Cancer Res.* 2020;26:3999–4009.
47. Sedykh SE, Prinz VV, Buneva VN, Nevinsky GA. Bispecific antibodies: design, therapy, perspectives. *Drug Des Devel Ther.* 2018;12:195–208.
48. Moek KL, Waaijer SJH, Kok IC, et al. ^{89}Zr-labeled bispecific T-cell engager AMG 211 PET shows AMG 211 accumulation in CD3-rich tissues and clear, heterogeneous tumor uptake. *Clin Cancer Res.* 2019;25:3517–3527.
49. Geiger M, Stubenrauch K-G, Sam J, et al. Protease-activation using anti-idiotypic masks enables tumor specificity of a folate receptor 1-T cell bispecific antibody. *Nat Commun.* 2020;11:3196.
50. van Brummelen EM, Huisman MC, De Wit-Van der Veen LJ, et al. ^{89}Zr-labeled CEA-targeted IL-2 variant immunocytokine in patients with solid tumors: CEA-mediated tumor accumulation and role of IL-2 receptor binding. *Oncotarget.* 2018;9:24737–24749.
51. Khalil DN, Smith EL, Brentjes RJ, Wolchok JD. The future of cancer treatment: immunomodulation, CARs and combination therapy. *Nat Rev Clin Oncol.* 2016;13:273–290.
52. Kircher MF, Gambhir SS, Grimm J. Noninvase cell-tracking methods. *Nat Rev Clin Oncol.* 2011;8:677–688.
53. Bansal A, Pandey MK, Demirhan YE, et al. Novel ^{89}Zr cell labeling approach for PET-based cell trafficking studies. *EJNMMI Res.* 2015;5:19.
54. Jung KO, Kim TJ, Yu JH, et al. Whole-body tracking of single cells via positron emission tomography. *Nat Biomed Eng.* 2020;4:835–844.
55. Jansen MH, Veldhuijzen van Zanten SEM, Van Vuurden DG, et al. Molecular drug imaging: ^{89}Zr-bevacizumab PET in children with diffuse intrinsic pontine glioma. *J Nucl Med.* 2017;58:711–716.
56. Lesniak WG, Chu C, Jablonska A, et al. A distinct advantage to intraarterial delivery of ^{89}Zr-bevacizumab in PET imaging of mice with or without osmotic opening of the blood-brain barrier. *J Nucl Med.* 2019;60:617–622.
57. Veldhuijzen-van Zanten SEM, De Witt Hamer PC, Van Dongen GAMS. Brain access of monoclonal antibodies as imaged and quantified by ^{89}Zr-antibody PET: perspectives for treatment of brain diseases. *J Nucl Med.* 2019;60:615–616.